Or-189

UCRL-51921

ESTIMATED REFRACTIVE INDEX AND SOLID DENSITY OF DT, WITH APPLICATION TO HOLLOW-MICROSPHERE LASER TARGETS

C. K. Briggs
R. T. Tsugawa
C. D. Hendricks
P. C. Souers

September 16, 1975

Prepared for U.S. Energy Research & Development Administration under contract No. W-7405-Eng-48

Printed in the United States of America
Available from
National Technical Information Service
U. S. Department of Commerce
5285 Port Royal Road
Springfield, Virginia 22151
Price: Printed Copy $___*; Microfiche $2.25

*Pages	NTIS Selling Price
1-50	$4.00
51-150	$5.45
151-325	$7.60
326-500	$10.60
501-1000	$13.60

Distribution Category
UC-21

LAWRENCE LIVERMORE LABORATORY
University of California/Livermore, California/94550

UCRL-51921

ESTIMATED REFRACTIVE INDEX AND SOLID DENSITY OF DT, WITH APPLICATION TO HOLLOW-MICROSPHERE LASER TARGETS

C. K. Briggs
R. T. Tsugawa
C. D. Hendricks
D. C. Souers

MS. date: September 16, 1975

Contents

ESTIMATED REFRACTIVE INDEX AND SOLID DENSITY OF DT, WITH APPLICATION TO HOLLOW-MICROSPHERE LASER TARGETS

by

C. K. Briggs, R. T. Tsugawa, C. D. Hendricks and P. C. Souers

Abstract

The literature values for the 0.55-μm refractive index N of liquid and gaseous H_2 and D_2 are combined to yield the equation

$$(N - 1) = [(3.15 \pm 0.12) \times 10^{-6}]\rho,$$

where ρ is the density in moles per cubic meter. This equation can be extrapolated to 300 K for use on DT in solid, liquid, and gas phases. The equation is based on a review of solid-hydrogen densities measured in bulk and also by diffraction methods. By extrapolation, the estimated densities and 0.55-μm refractive indices for DT are as follows:

State	T (K)	Density (moles/m^3)	Refractive index
Solid	4.2	0.053	1.17
Solid	19.71[a]	0.051	1.16
Liquid	19.71[a]	0.0446	1.14

[a]Triple point.

Radiation-induced point defects could possibly cause optical absorption and a resulting increased refractive index in solid DT and T_2. The effect of the DT refractive index in measuring glass and cryogenic DT laser targets is also described.

Introduction

A possible source of energy in the twenty-first century is laser-induced hydrogen fusion.[1-3] The experimental laser targets that are currently in use are hollow glass microspheres filled with DT gas,[4-6] whereas future laser targets are expected to be either liquid or solid microspheres--first hollow and ultimately solid--of DT itself. Because the basic method of inspecting transparent laser targets is optical, the refractive index of hydrogen will be of continuing importance. In anticipation of cryogenic targets, we are initiating an experimental program on the properties of cryogenic DT. We are also reviewing a number of topics of current interest in the area of cryogenic hydrogen.[7-9]

Literature Survey of Hydrogen Refractive Indices

The literature data are largely derived from two papers,[10,11] which are partly summarized in the National Bureau of Standards cryogenic review.[12] The first paper[10] reports measurements of the refractive index of gaseous and liquid H_2 at 0.5462 μm by interferometry at temperatures of between 15 and 298 K and at pressures of up to 23 MPa. The second paper[12] concerns data for liquid D_2 (assumed normal*) at 0.5461 μm obtained by computations based on earlier refractive index[12,13] and density data.[12,14] Estimated liquid D_2 values at temperatures from 18.7 to 30 K are also given for two other wavelengths: 0.3200 μm, for which (N - 1) is 5.4% higher than at 0.5461 μm, and 0.6328 μm, for which (N - 1) is 0.7% lower.[11] Several other sources of data also exist.[15-17] We have found no data on solid hydrogen in the literature.

Empirical Refractive Index-Density Relation

Most estimates of the refractive index are based on the Lorentz-Lorenz function,[18] which, however, is extremely sensitive to errors of measurement. Instead, we plot in Fig. 1 the refractive index of H_2 and D_2 at 0.55 μm as a function of density in moles per cubic meter. We find an essentially linear relationship over the temperature range 15 to 298 K and for both gas and liquid phases.

The further generality of this refractive index-density relationship, at least

---

*Symmetric (sym or para) H_2 has 100% of its molecules in even-numbered rotational levels. At low temperatures, sym-H_2 is the natural form and occupies the J = 0 rotational level, where J is the rotational quantum number. If sym-H_2 is brought quickly to room temperature, molecular symmetry allows only fast $\Delta J = \pm 2$ transitions, and the symmetric J = 2 level will be partly occupied. Over a period of weeks, forbidden $\Delta J = \pm 1$ transitions will occur, causing population of the antisymmetric (asym) J = 1 and J = 3 levels. Normal hydrogen (nH_2) is the room-temperature equilibrium mixture with a population of 25.1% sym (even-numbered J) and 74.9% asym (odd-J). The D_2 mentioned above is assumed to be normal, with 66.7% sym-D_2 and 33.3% asym-D_2. If quickly cooled, nH_2 and nD_2 will have their asymmetric components metastably trapped in the J = 1 levels.

The term "equilibrium" (e) refers to the equilibrated sym-asym mixture at any temperature other than room temperature. The species HD, DT, and HT are expected to equilibrate quickly by $\Delta J = \pm 1$ transitions allowed in molecular hydrogen with mixed isotopes. The species T_2, DT, and HT are expected to also equilibrate quickly (e.g., an hour) due to the catalyzing effects of the tritium β particle.[8,9]

Solid hydrogen is unusual in that the di-atomic molecules are scarcely affected by the crystal fields, and J remains a good quantum number.

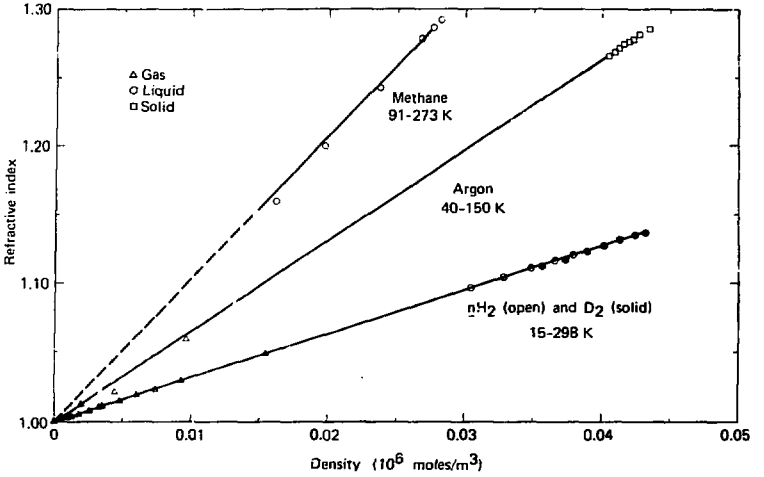

Fig. 1. Refractive index vs. density for methane, argon, $\underline{n}H_2$, and D_2.

for simple compounds, is shown by additional points in Fig. 1 for argon and methane, which can be summarized as follows:

Species	State	T (K)	Wavelength (μm)
Argon[19]	Gas	125-150	0.5893
Argon[19]	Liquid	86-145	0.5893
Argon[20,21]	Solid	40-84	0.5893
Methane[22]	Gas[a]	298	0.5462
Methane[19]	Liquid	91-185	0.5893

[a]At a pressure of 0.1 MPa.

Figure 1 yields a second bonus. It appears that the H_2 and D_2 data fall on the same line. We shall analyze this more closely below, but we can immediately postulate a simple equation for all hydrogen isotopes, at any temperature, and for any phase:

$$(N - 1) = A'\rho, \tag{1}$$

$$A' = (3.15 \pm 0.12) \times 10^{-6}\ m^3/mole, \tag{2}$$

where N is the refractive index at 0.55 μm and ρ is the density in moles per cubic meter. Calculations with this equation give refractive indices for liquid H_2 that are 1.4% low and for gaseous H_2 that are 1% high.

From the data presented later, we estimate an error bar of ±4% for (N - 1) in covering all the hydrogen isotopes.

Corrections to the Linear Relationship

The relationship of refractive index and density may not be exactly linear. The accuracy of measurements is difficult to determine but may be considered as ±(0.1 to 0.2%) for $(N - 1)$ and ±(0.1 to 0.5%) for density.[10] This leads to accuracy estimates of ±(0.2 to 1%) for the linear coefficient in Eq. (1).

We have attempted to improve Eq. (1) by determining two virial coefficients. The first step in accomplishing this is to calculate the coefficient $A' \equiv (N - 1)/\rho$ for all H_2 and D_2 data, distinguishing between liquid and gas, and between sym and normal states. The results are shown in Fig. 2. We may immediately distinguish two H_2 gas lines, one for 30 to 100 K and the other for 298 K, with nH_2 and sym-H_2 points being indistinguishable. We now expand Eq. (1) to include a second virial coefficient,

$$A' = A + B\rho, \tag{3}$$

where A' is defined as $(N - 1)/\rho$ in Eq. (1) and ρ is the density in moles per cubic meter. From Fig. 2, we obtain the following coefficients for H_2 gas:

T (K)	A (m^3/mole)	B [(m^3/mole)^2]
30-100	3.116×10^{-6}	1.857×10^{-12}
298	3.127×10^{-6}	1.534×10^{-12}

The data of Fig. 2 suggest a slight isotope effect, since A' for D_2 lies below the values for H_2. The slope B remains about the same, but the intercept A is 0.038 m^3/mole lower for D_2 than for H_2. For cold T_2 gas, we extrapolate an A value of 3.040×10^{-6} m^3/mole, which yields an expected refractive index about 3% lower than the value generated by Eq. (1). Hence we have given a ±4% spread to Eq. (1).

The data for the liquid are not so well behaved. Figure 3 shows the coefficient A' as a function of temperature for the liquids sym-H_2, nH_2, and D_2 (assumed normal). The sym-H_2 data show a strange drop near the critical point, which has not been explained as yet. Again, the values are lower for D_2 than for H_2. We roughly extrapolate the data for higher mass and to lower temperatures to obtain

Liquid:

$$A' = [3.190 - 0.0175\ (M - 2)] \times 10^{-6}\ m^3/\text{mole}. \tag{4}$$

Solid:

$$A' = [3.195 - 0.015\ (M - 2)] \times 10^{-6}\ m^3/\text{mole}. \tag{5}$$

Here M is the molecular weight of the appropriate hydrogen species (to the nearest integer).

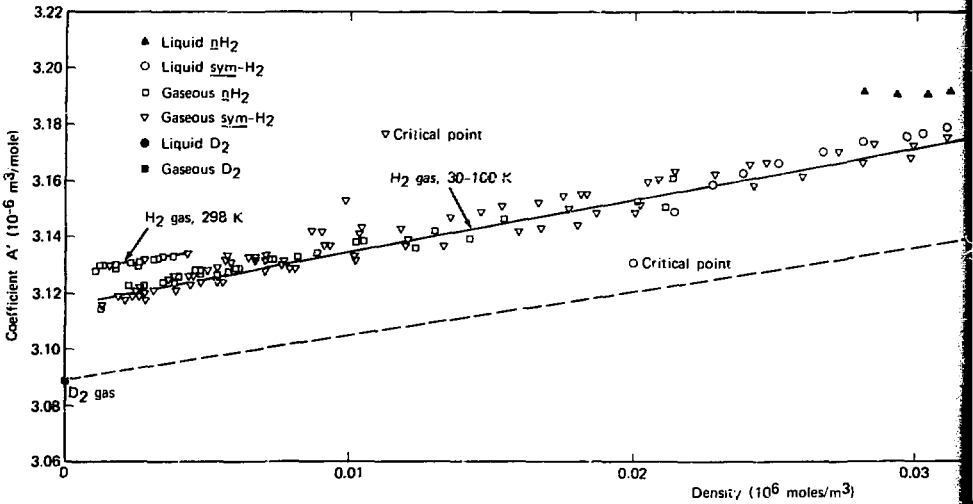
Liquid nH2
Liquid sym-H2
Gaseous nH2
Gaseous sym-H2
Liquid D2
Gaseous D2
Critical point
H2 gas, 30-100 K
H2 gas, 298 K
Critical point
D2 gas
Coefficient A' (10-6 m3/mole)
Density (10^6 moles/m3)
3.22
3.20
3.18
3.16
3.14
3.12
3.10
3.08
3.06
0
0.01
0.02
0.03

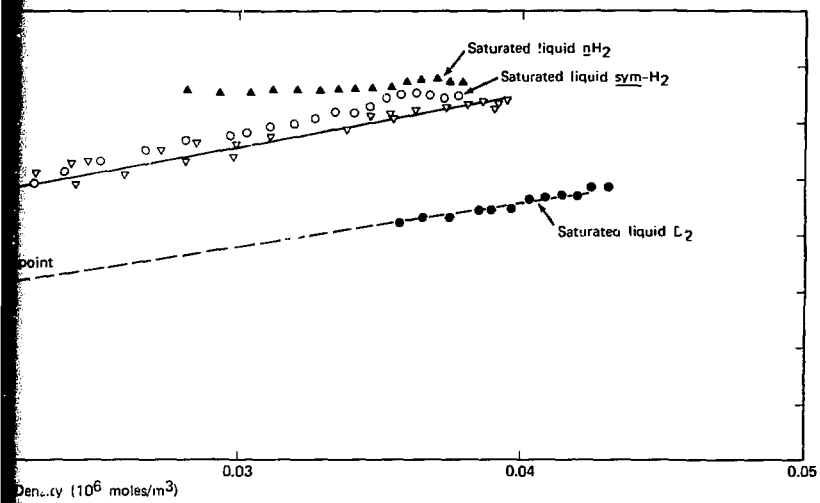

Fig. 2. Coefficient A' as a function of density.

2

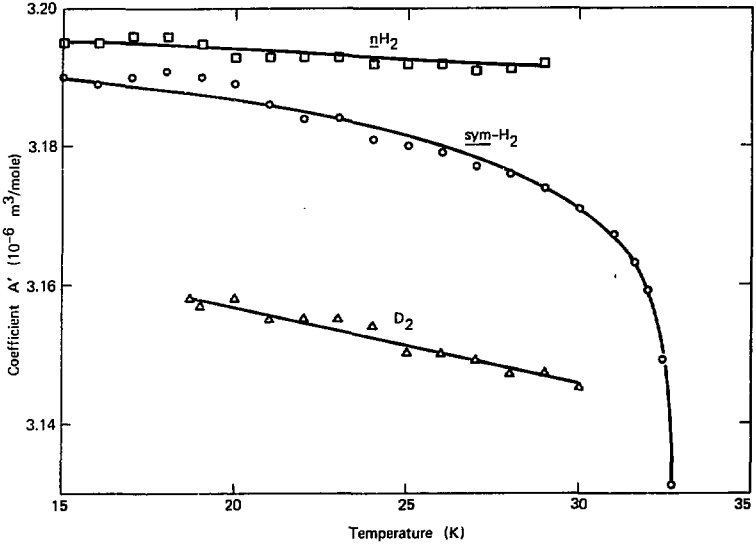

Fig. 3. Coefficient A' as a function of temperature for sym-H_2, nH_2, and D_2.

Densities of Liquid and Solid Hydrogen

The liquid densities for the hydrogens from the triple points to 25 K can be taken from a previous compilation.[9] The data are shown in Fig. 4 and Table 1.

It now remains to consider the literature data for solid hydrogen, which forms in a hexagonal close-packed (hcp) structure on freezing at the triple point.[24] Density determinations have been made primarily by two methods: bulk densities reported as molar volumes, and densities determined from diffraction measurements of crystal structure. These two methods are reviewed separately in this report.

BULK DENSITIES

Four separate studies have been carried out.[24-28] The most basic approach was taken by Megaw, who first measured solid H_2 and D_2 densities in 1939. She filled a known volume with solid hydrogen and measured the amount by subliming to a PVT apparatus. The technique was cross-checked with solid helium of known density.[25] The other major approach to this measurement is to determine the phase diagram and latent heat of fusion and then calculate the volume change on freezing by the Clausius-Clapeyron equation.[26,29] From a knowledge

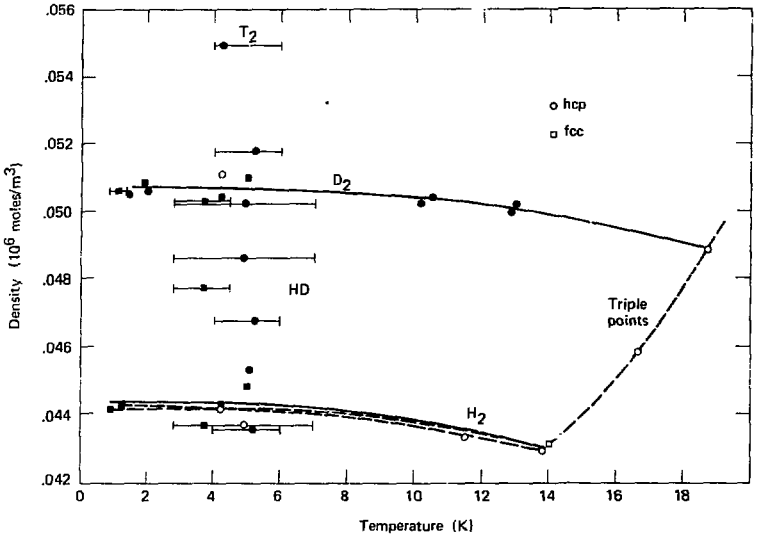

Fig. 4. Densities of the hydrogen isotopes in the solid state as a function of temperature. The open symbols represent data obtained in bulk determinations; the solid symbols are points for data obtained in crystal-structure determinations.

Table 1. Lattice parameters of solid hydrogen.[a]

Species	hcp a	hcp c	hcp c/a	fcc a	Diffraction method	Reference
H_2	3.76	6.11	1.62	5.31	x-ray	32[b]
HD	3.68	6.06	1.66	--	x-ray	31
	3.64	5.95	1.63	5.18	Electron	34
D_2	3.59-3.62	5.83-5.88	1.61-1.64	5.07-5.08	x-ray	37[b]
					Neutron	38[b], 39[b]
T_2	3.47	5.80	1.67	--	x-ray	31, 40

[a]Lattice parameters in angstroms.

[b]Considered best data.

of the density of the liquid, the corresponding density of the solid may be calculated.

Bulk-density data are available for H_2 at 4.2 K[25] and at the triple point,[26] for HD at the triple point,[26] and for D_2 at 4.2 K[25] and at the triple point.[26]

CRYSTAL-STRUCTURE DENSITIES

Much work has been done in this field in studying the transition from hexagonal close-packed structure to face-centered cubic structure (hcp → fcc) that takes place as solid hydrogen is cooled to 2 to 4 K. The transition is first order, but the volume change is[30] only 0.5%, and the densities of the two phases are interchangeable within experimental error. The *sym-asym* ratios also appear to have no measurable effect on density.

The methods used include x-ray, electron, and neutron diffraction. The phases have been studied at the nominal temperatures listed below.

	hcp Structure		fcc Structure	
Species	T (K)	Ref.	T (K)	Ref.
H_2	1.3-7	31-36	0.9-5	32-36
HD	2.8-7	31,34	2.8-4.5	34
D_2	1.4-13	31,34-39	1-5	33,35, 38,39
T_2	4.2	31,40	-	-

The best data, in our opinion, come from certain of the x-ray diffraction[32,38] and neutron-diffraction data[37,39] and cover only H_2 and D_2. The range of lattice parameters for both crystal structures is shown in Table 1. The hcp structure corresponds almost exactly to the classical close packing of spheres, which has a c/a ratio[41] of 1.633. The densities may be calculated from the lattice parameters, recalling that the hcp structure has two lattice points per cell[41] and the fcc structure has four.[42]

All the bulk and crystal structure densities described above are now combined as a function of temperature in Fig. 4. Many of the crystal structure points have considerable error bars of temperature uncertainty. The two broken H_2 lines represent the results of two thermodynamic theories, and the agreement is quite good.[43,44]

We have derived empirical formulas for the data of Fig. 4. The curvature of the D_2 data requires the empirical form

$$\rho = \rho_0 - CT^3, \tag{6}$$

where ρ is the solid density in moles per cubic meter, ρ_0 the density at 0 K, T is the temperature, and C is a constant. The solid lines for H_2 and D_2 in Fig. 4 are the easily derived forms for Eq. (6). The coefficients ρ_0 and C are listed for H_2 and D_2 in Table 2 with the densities at 4.2 K and at the triple point. For HD, however, only data at the triple point are usable; the scatter at low temperatures makes estimation of ρ_0 impossible. If we interpolate between the values of ρ_0 and C for H_2 and D_2, we obtain a fit that is quite reasonable.

For heavier molecules than D_2, however, the uncertainties become extreme. There is only one point for T_2 at 4.2 K, with a possible temperature uncertainty of 2 degrees above liquid helium temperatures.

Table 2. Densities and refractive indices of liquid and solid hydrogen.[a,b]

Species	Triple point (K)	Constant C ($\times 10^{-7}$)	Density (10^6 moles/m^3)				Refractive index at 0.55 μm		
			Solid, 0 K, ρ_0	Solid, 4.2 K	Solid, triple point	Liquid, triple point	Solid, 4.2 K	Solid, triple point	Liquid, triple point
J = 0 H_2	13.803	4.78	(0.0443)	0.0443	0.04291	0.03821	(1.142)	(1.137)	1.122
nH_2	13.957				0.04301	0.03830		(1.137)	1.122
HD	16.604	(3.84)	(0.0476)	0.048	0.04579	0.04062	(1.15)	(1.146)	(1.129)
J = 0 D_2	18.691	2.90	(0.0507)	0.0507	0.04859	0.04299	(1.160)	(1.154)	(1.136)
nD_2	18.71				0.04883	0.04317		(1.155)	1.136
DT	(19.71)	(2.5)	(0.053)	(0.053)	(0.051)	(0.0446)	(1.17)	(1.16)	(1.140)
eT_2	20.62	(2.4)	(0.055)	(0.055)	(0.053)	0.04539	(1.17)	(1.17)	(1.142)

[a] Data from Refs. 31 and 45.

[b] Estimated values are shown in parentheses.

Even so, the density of 0.0549×10^6 moles/m^3 seems high.* Solid T_2 must either shrink more than D_2 on warming to the triple point (i.e., must have a larger value of C) or must exhibit a large shrinkage on freezing. We have taken a ρ_0 value of 0.055×10^6 moles/m^3 for T_2, essentially the 4.2 K value, and estimated a C value of $(2.4 \pm 1.4) \times 10^{-7}$ mole/m^3-K, just below that of D_2. This yields an estimated density at the triple point of $(0.053 \pm 0.001) \times 10^6$ moles/m^3. This large uncertainty is also shown by the error bar for the molar volume of the solid at the triple point for T_2. Once ρ_0 and C values are estimated, corresponding values are obtained for DT by interpolation. These are listed in Table 2.

By using Eq. (6) plus the isotopic coefficients listed in Table 2, we can estimate the solid densities from 0 K to the triple point. These estimates are good for either the hcp or fcc structures and for any sym-asym mixture, because small changes are submerged in the errors of estimation. The resulting solid and liquid densities at 4.2 K and the triple points are also listed in Table 2.

Once densities are known, the refractive indices of liquid and solid hydrogen can be calculated from Eqs. (1), (4), and (5). The resulting refractive indices at 4.2 K and at the triple points are listed in Table 2. The refractive indices of the solids assume no new effects due to the radiation from the tritium. Radiation-induced point defects, however, could conceivably cause absorption and an increased refractive index in the visible portion of

*This value is obtained from the hcp x-ray lattice parameters.[31] However, the previous Soviet value of 0.0537×10^6 moles/m^3, which was erroneously derived for an assumed tetragonal structure,[40] has been cited in NBS-641.[45] This value leads to a freezing shrinkage volume more in line with the lower-mass hydrogen isotopes, but we report the Soviet data in the form the researchers considered to be final.

Table 3. Specific volumes and freezing shrinkages for liquid and solid hydrogen.[a,b]

Species	Molecular weight (g/mole)	Triple point (K)	Specific volume (10^{-6} m^3/mole) Solid, 0 K	Solid, triple point	Liquid, triple point	Freezing shrinkage volume	Freezing shrinkage (%)
J = 0 H_2	2.016	13.803	(22.57)	23.30	26.173	-2.873	-11.0
$\underline{n}H_2$		13.957		23.25	26.108	-2.858	-11.0
HD	3.023	16.604	(21.03)	21.84	24.62	-2.78	-11.3
J = 0 D_2	4.029	18.691	(19.72)	20.58	23.262	-2.682	-11.5
$\underline{n}D_2$		18.71		20.48	23.162	-2.682	-11.6
DT	5.032	(19.71)	(18.8)	(19.5)	(22.4)	(-3.0)	(-13)
$\underline{e}T_2$	6.034	20.62	(18.2)	(18.9)	22.03	(-3.1)	(-14)

[a]Data from Refs. 31 and 45.

[b]Estimated values are shown in parentheses.

the spectrum. There is no way to estimate such effects at this time. It appears important that an optical spectrum should be measured for DT to ascertain possible problems of laser light absorption.

We now invert the liquid and solid densities into specific volumes, which are listed for 4.2 K and the triple points in Table 3. The specific volumes at 0 K and at the triple points are also plotted in Fig. 5 as a function of molecular weight, so that the effect of increasing molecular weight may be observed. The experimental densities of Table 2 and specific volumes of Table 3 and Fig. 5 are the recently recommended values of the National Bureau of Standards.[45]

Table 3 shows that H_2, HD, and D_2 all contract about 11% with a slight increase with molecular weight. However, estimated DT and T_2 shrinkage values are approximately 13 and 14%, respectively. This effect is also shown by the widening of the gap between the molar volumes of the solid

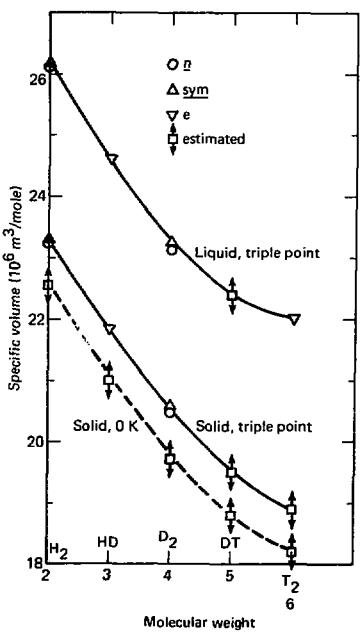

Fig. 5. Specific volumes of the liquid and solid hydrogens.

and the liquid at the triple point in Fig. 5. The larger shrinkage estimates are due solely to the single Soviet T_2 data point[31] at 4.2 K. It would be quite interesting to measure the DT and T_2 freezing shrinkage volumes to see if they are indeed larger than expected from the lighter hydrogen isotopes.

The shrinkage is also quite important as regards laser-target fabrication. It is thought that hollow DT microspheres may be the targets at 10-kJ laser energies.[1-3] Recently, such shells of hollow H_2 have been prepared by the Rayleigh liquid-jet method.[46] Such hollow liquid microspheres would be injected into a vacuum for laser firing. Sublimation in the vacuum would cause the microsphere to freeze from the outside in. The resulting shrinkage would set up strains that could conceivably shatter the frozen bubble. Since nucleation of the freezing would probably not be symmetrical, the shrinkage might also cause considerable distortion of the symmetrical microsphere. For these reasons, the details of the DT freezing process will be of great importance in laser-target fabrication.

The Low-Temperature hcp → fcc Transformation

Heat-capacity measurements on solid H_2 and D_2 show a component below 11 K that does not decline to zero according to the usual Debye curve.[47] This is due to the presence of the frozen-in metastable J = 1 species. When the J = 1 species is more than 60% of the total, the heat capacity shows a spike in the vicinity of 2 K, which was called, when first discovered, the λ anomaly.[48]

By 1968, a large amount of data could be correlated. The results of x-ray diffraction measurements on bulk crystals show that the hcp structure of hydrogen formed at the triple point changes at the λ anomaly to fcc.[35,49] This occurs in H_2 and D_2 only for J = 1 greater than about 60%. For J = 1 less than 60%, the hcp structure remains[50] to at least 0.2 K. The phase transformation is first order, with a volume change[30] of 0.5%. It demonstrates hysteresis, with the fcc structure becoming more stable with each thermal recycle, until heating to 12 K is required to fully reconstitute the hcp structure. This hysteresis is greater for D_2 than for H_2 and increases as the J = 1 component increases toward 100%. The transition temperature also increases linearly with the percent of the J = 1 component, with extrapolated 100% values[35] being 2.8 K for H_2 and 3.8 K for D_2. Supporting evidence for the phase transformation is also seen in the results of measurements by neutron diffraction,[39] infrared spectroscopy,[51] and nuclear magnetic resonance.[52]

Electron-diffraction studies on 100- to 1000-Å films of solid hydrogen show, however, that the fcc form is more easily generated in films than in bulk crystals.[33,34] Films of $n\underline{H}_2$, HD, and $n\underline{D}_2$ first freeze on the substrates in hcp form with the c-axis perpendicular to the substrate surface. Conversion to the fcc form occurs in the range 4.5 to 5 K. The conversion of HD,[34] surely a state where the J = 1 species is close to zero, is quite unexpected.

It has long been believed that an ordering of rotational moments is involved in the λ anomaly, although the actual physical arrangement is not well understood. The most picturesque analogy is to imagine the $J = 1$ rotational moments lining up in an "antiferromagnetic" structure.[53,54] A rotational moment may flip, and the excitation may travel down the crystal lattice in a wavelike manner. Such an excitation is assumed to take and give energy in a quantized manner. It is called a "libron," by direct analogy with spin-wave "magnons" in antiferromagnetic crystals. For this reason, the fcc structure is called the "ordered" state of hydrogen, and the hcp structure the "disordered."

It is thought that some degree of rotational-moment ordering may occur even in the hcp forms that exist to 0.2 K when the $J = 1$ species is less than 60% in bulk samples.[55] As the percentage of the $J = 1$ species increases, the force for alignment increases rapidly until the actual crystal transformation occurs.[35] Thin films may become ordered more easily because of the forces from the substrate and the small amount of hydrogen to be rearranged. Several studies using Raman spectroscopy are currently under way in order to ascertain the true ordered structure by studying the librons.[56,57]

The hcp → fcc transformation does not appear to be of great importance from an applied point of view. By extrapolating the 100% $J = 1$ transition temperatures for H_2 and D_2, one might expect a transformation of bulk frozen DT and T_2 above 4.2 K. It may even occur at higher temperatures for DT plated onto the sides of a glass microsphere, since this may approximate the thin-film behavior. However, the tritium β particle is likely to catalyze rotational transitions to the $J = 0$ level in less than an hour.[58,59] The low-temperature equilibrium mixture of eD_2–DT–eT_2 will have a low percentage of $J = 1$ molecules to induce ordering. Perhaps the only transformation property that might affect laser-target fabrication is the volume change, which will place an additional stress on the frozen microsphere.

Light-Interference Measurements on Glass Laser Targets

It has been mentioned that current laser-fusion targets are glass microspheres that have been selected for uniform wall thickness by light interference[4-6] and filled with DT. The circular fringes may be analyzed by a refractive ray-trace program that yields the average wall thickness, provided the refractive index of the glass is known. Stone showed that such wall-thickness measurements are heavily influenced by the refractive index of the DT fill gas inside the microsphere.[60] Weinstein has devised an improved wall-thickness measurement method, employing white light, that also depends on knowing the refractive index of DT gas.[61]

The full refractive ray-trace program[5,62] is too complex to present here, but a simple theory serves to show the physical principles involved.

The interferometer is composed of a reference arm and the sample arm containing the hollow glass microsphere. A light beam is

split into two parts, one entering each arm. The beams in each arm travel almost identical path lengths (including reflection at identical mirrors), reconverge, and interfere. Microscope lenses are included in each interferometer arm since laser targets are only 50 to 100 μm in diameter.

A schematic for the simple light interference model is shown in Fig. 6. All lengths are dimensionless, having been divided by the true outer radius r_1. The ray in Fig. 6 proceeds from left to right, is reflected at the mirror, and returns. The index of refraction is 1.000 for the air, N' for the microsphere glass, and N" for the DT gas inside the microsphere. Other lengths, in dimensionless units, are P, the planar radius to an arbitrary ray; L, the wall thickness; and (1 - L), the inner radius.

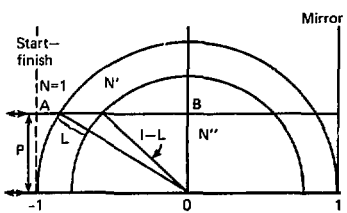

Fig. 6. Schematic of the simple theory of light interference.

For the arbitrary ray, we need only consider the physical distances through air, glass, and gas from point A to B and multiply each length by the appropriate refractive index. The fiducial ray for the microsphere is the x-axis ray, which passes through the least amount of glass. We assume that a glass spacer has been inserted in the reference arm of the interferometer to bring the optical path difference between the reference arm x-axis ray and microsphere x-axis ray to zero. We can then ignore the reference rays, with which the interference in fact occurs, and consider only the relation of the microsphere rays.

The optical path length of the x-axis microsphere ray, S_0, from start to finish, is

$$S_0 = 4\,[N'L + N''(1 - L)]. \qquad (7)$$

The corresponding optical path length of the arbitrary ray, S, of planar radius P is

$$S = 4\left(\left[1 - (1 - P^2)^{\frac{1}{2}}\right] + N'\left\{(1 - P^2)^{\frac{1}{2}} - [(1 - L)^2 - P^2]^{\frac{1}{2}}\right\} + N''\,[(1 - L)^2 - P^2]^{\frac{1}{2}}\right). \qquad (8)$$

The two microsphere rays will reach the finish line at different times, since the arbitrary ray has been slowed down by passage through more glass. The phase difference between the two rays is obtained by subtracting Eq. (7) from Eq. (8). For physical simplicity, we also expand the square-root terms to a two-term binomial series expression as follows:

$$(1 - P^2)^{\frac{1}{2}} \approx 1 - \frac{P^2}{2} \qquad \text{for } P \ll 1. \qquad (9)$$

By carrying out the indicated operations, we obtain the optical-path-length difference ΔS:

$$\Delta S = \frac{2P^2}{(1 - L)}\,(N' - 1)L - (N'' - 1). \qquad (10)$$

If the optical-path-length difference in Eq. (10) is multiplied by the true outer radius r_1, the resulting length may be compared with the wavelength of the observing light. Constructive interference at the arbitrary planar radius P will occur if

$$\Delta S = \frac{m\lambda}{r_1}, \tag{11}$$

where λ is the wavelength of the observing light and m is an integer. Hence we expect a series of interference rings, representing different orders m. Equation (10) shows that the optical-path-length difference increases parabolically, so that higher order interference fringes become more crowded as one progresses outward from the center of the microsphere. Since Eq. (10) is derived from an approximation in which $P \ll 1$, one might expect the exact ΔS to rise even more steeply. Physically, however, one cannot display a fringe in less than a half-wavelength of planar radius (i.e., $\partial\Delta S/\partial P < 1$). One expects the fringes to possibly fade out near the edge.

The refractive ray-trace program[5,67] yields an optical-path-length difference ΔS that rises with the planar radius P more steeply than the parabolic function of Eq. (10). Refraction also reduces the glass paths and increases the air-gas distances, so that the code-predicted behavior is better described by the form

$$\Delta S = \frac{1.6\ P^2}{(1 - L)}\ [(N' - 1)L - 1.4(N'' - 1)]. \tag{12}$$

Equation (12) shows that the presence of DT gas inside the microsphere will lower the optical path difference. This is because the arbitrary ray passes through less DT gas than does the x-axis ray and hence gains in time. A typical laser target is of glass with refractive index 1.50 and has an L value of 0.02. If the microsphere were filled to 10^3 moles/m^3 (2.5 MPa or 360 psi at 300 K), the DT gas refractive index, N", according to Eqs. (1) and (2), would be 1.00315. In Eq. (12), the second term is almost the size of the first. The total optical path is reduced by almost half, and the fringes are pushed outward on the face of the microsphere. If DT gas could be added without breaking the microsphere, the eventual result would be the condition

$$(N' - 1)L = 1.4(N'' - 1), \tag{13}$$

in which no fringes are obtained because the glass path and the DT path just cancel one another. For the microsphere example above, this would occur for a pressure of about 6 MPa, which would probably break the glass walls.

Interferometry on Frozen DT Microspheres

It is interesting to consider the corresponding light interference pattern for a frozen hollow DT microsphere. At 4.2 K, the refractive index of the walls, N', is, by the estimate of Table 2, only 1.17. The vapor pressure at 4.2 K is estimated to be about 2.4×10^{-10} Pa (1.8×10^{-12} Torr)[63] so that the internal gas refractive index is 1.000. The term (N' - 1) in Eq. (12) is one-third the magnitude of that of glass,

and the fringes will be at least $(3)^{\frac{1}{2}}$ farther out for the same dimensions. Only a fairly thick microsphere will show even a first fringe. For a diameter of 100 μm and 0.55-μm light, the thickness L must be greater than 0.024 μm to accumulate even one half-wavelength of optical-path-length difference.

At the triple point, liquid DT has an estimated refractive index N' of 1.14 (Table 2) and an estimated equilibrium vapor pressure of 1.94×10^4 Pa (145.7 Torr).[45] The vapor pressure yields a density of 119 moles/m^3 and an estimated refractive index N" of 1.00037. Equation (12), corrected for the equilibrium atmosphere outside the microsphere as well, becomes

$$\Delta S = \frac{1.6\ P^2}{(1 - L)}(N' - N'')L. \qquad (14)$$

The optical-path-length difference is now only 28% that of the glass microsphere; the fringes, if any, move out a little further. The path-subtraction effect of Eq. (13) is reduced in importance by roughly the factor L. This is because the sum of the DT gas outside and inside results in an almost constant path-length correction to ΔS.

It is apparent that the interferometry of small DT microspheres can be hampered by the very small difference in predicted refractive index between the liquid and the solid. Higher laser energies will lead to the use of larger microspheres, which will be easier to examine. The two-arm method of interference may not be practical at low temperatures for a moving-target microscope. Single-arm interferometers exist and will be more stable in a cryostat. The use of multiple reflections to build up optical path-length difference in the Fabry-Pérot etalon may be useful.[64] Also of interest is the refractive method of Reedy of this Laboratory,[65,66] in which parallel light is refracted by the microsphere and collected by a lens with a known, stopped aperture. A black ring is seen at the microsphere edge, and light interference is not required. However, the single pass of the light through the low-index solid DT will not produce refraction at very large angles, and a sensitivity problem will also appear.

Acknowledgment. We wish to thank J. Emmett of LLL for his continuing interest in the properties of cryogenic DT.

References

1. J. Nuckolls, L. Wood, A. Thiessen, and G. Zimmerman, Nature 239, 193 (1972).

2. J. Nuckolls, J. Emmett, and L. Wood, Physics Today 26(8), 46 (August 1973).

3. J. Emmett, J. Nuckolls, and L. Wood, Scientific American 230(6), 24 (June 1974).

4. P. C. Souers, R. T. Tsugawa, and R. R. Stone, Rev. Sci. Instr. 46, 682 (1975).

5. R. R. Stone, D. W. Gregg, and P. C. Souers, J. Appl. Phys. 46, 2693 (1975).

6. P. C. Souers, R. T. Tsugawa, and R. R. Stone, Fabrication of the Glass Microbubble Laser Target, Lawrence Livermore Laboratory, Rept. UCRL 51609 (1974).

7. P. C. Souers, R. G. Hickman, W. Z. Wade, and R. T. Tsugawa, A Simple Model of D_2-DT-T_2 Equilibrium at Cryogenic Temperatures, Lawrence Livermore Laboratory, Rept. UCRL 51681 (1974).

8. P. C. Souers, R. G. Hickman, W. Z. Wade, and R. T. Tsugawa, Estimated Infrared Spectra of Cryogenic D_2-DT-T_2, Lawrence Livermore Laboratory, Rept. UCRL-51674 (1974).

9. C. K. Briggs, R. G. Hickman, R. T. Tsugawa, and P. C. Souers, Estimated Viscosity, Surface Tension and Density of Liquid DT from the Triple Point to 25 K, Lawrence Livermore Laboratory, Rept. UCRL-51827 (1975).

10. D. E. Diller, J. Chem. Phys. 49, 3096 (1968).

11. G. E. Childs and D. E. Diller, Adv. Cry. Eng. 15, 65 (1969).

12. H. M. Roder, G. E. Childs, R. D. McCarty, and P. E. Angerhofer, Survey of the Properties of the Hydrogen Isotopes Below Their Critical Temperature, National Bureau of Standards Technical Note 641 (August 1973), Section 7-1.

13. T. Larsen, Z. Physik 100, 543 (1936).

14. R. Prydz, The Thermodynamic Properties of Deuterium, National Bureau of Standards, Rept. 9276 (1967).

15. H. E. Johns and J. O. Wilhelm, Can. J. Res. 15, 101 (1937).

16. R. J. Corruccini, Refractive Index and Dispersion of Liquid H_2, National Bureau of Standards Technical Note 323 (1965).

17. A. V. Belonogov and U. M. Gorbunkov, Instruments and Experimental Techniques, No. 3, 664 (May-June, 1965).

18. F. A. Jenkins and H. E. White, Fundamentals of Optics, 3rd ed. (McGraw-Hill, New York, 1967), p. 258.

19. C. P. Abbiss, C. M. Knobler, R. K. Teague, and C. J. Pings, J. Chem Phys. 42, 4145 (1965).

20. E. R. Dobbs, B. F. Figgins, G. O. Jones, D. C. Piercey, and D. P. Riley, Nature 198, 483 (1956).

21. A. J. Eatwell and G. O. Jones, Phil. Mag. 10, 1059 (1964).

22. H. E. Watson and K. L. Ramaswamy, Proc. Roy. Soc. (London) A156, 144 (1936).

23. F. A. Jenkins and H. E. White, Fundamentals of Optics, 3rd ed. (McGraw-Hill, New York, 1967), p. 481.

24. Reference 12, Sections 2.1-2.2.

25. H. D. Megaw, Phil. Mag. 28, 129 (1939).

26. H. W. Woolley, R. B. Scott, and F. G. Brickwedde, J. Res. Natl. Bur. Std. 41, 379-475 (1948).

27. R. F. Dwyer, G. A. Cook, O. E. Berwaldt, and H. E. Nevins, J. Chem. Phys. 43, 801 (1965).

28. G. A. Cook, R. F. Dwyer, O. E. Berwaldt, and H. E. Nevins, J. Chem. Phys. 43, 1313 (1965).

29. W. J. Moore, Physical Chemistry, 3rd ed. (Prentice-Hall, Englewood Cliffs, N.J., 1963), p. 104.

30. J. Jarvis, D. Ramm, and H. Meyer, Phys. Rev. Letters 18, 119 (1967).

31. V. S. Kogan, A. S. Bulatov, and L. F. Yakimenko, Soviet Physics--JETP 19, 107 (1964).

32. R. L. Mills and A. F. Schuch, Phys. Rev. Letters 15, 722 (1965).

33. A. E. Curzon and A. J. Mascall, Brit. J. Appl. Phys. 16, 1301 (1965).

34. O. Bostanjoglo and R. Kleinschmidt, J. Chem. Phys. 46, 2004 (1967).

35. A. F. Schuch, R. L. Mills, and D. A. Depatie, Phys. Rev. 165, 1032 (1968).

36. A. S. Bulatov and V. S. Kogan, Soviet Physics--JETP 27, 210 (1968).

37. K. F. Mucker, S. Talhouk, P. M. Harris, D. White, and R. A. Erickson, Phys. Rev. Letters 15, 586 (1965).

38. A. F. Schuch and R. L. Mills, Phys. Rev. Letters 16, 616 (1966).

39. K. F. Mucker, P. M. Harris, and D. White, J. Chem. Phys. 49, 1922 (1968).

40. V. S. Kogan, B. G. Lazarev, and R. F. Bulatova, Soviet Physics--JETP 10, 485 (1960).

41. C. Kittel, Introduction to Solid State Physics, 2nd ed. (Wiley, New York 1960), p. 35.

42. Ibid., p. 26.

43. G. Ahlers, Some Properties of Solid Hydrogen at Small Molar Volumes, Lawrence Radiation Laboratory, Rept. UCRL-10757 (1963).

44. Reference 12, Table 3-1.

45. Reference 12, Section 11.

46. C. A. Foster, C. D. Hendricks, and R. J. Turnbull, Appl. Phys. Letters 26, 580 (1975).

47. Reference 12, Section 4.

48. R. W. Hill and B. W. A. Ricketson, Phil Mag. 45, 727 (1954).

49. R. L. Mills, A. F. Schuch, and D. A. Depatie, Phys. Rev. Letters 17, 1131 (1966).

50. R. W. Hill, B. W. A. Ricketson, and F. Simon, in Conférence de Physique des Basses Temperatures, Paris, 1955 (Institute International de Froid, Paris, 1955), No. 76, p. 317, cited in Ref. 3.

51. M. Clouter and H. P. Gush, Phys. Rev. Letters 15, 200 (1965).

52. F. Reif and E. M. Purcell, Phys. Rev. 91, 63 (1953).

53. A. B. Harris, J. Appl. Phys. 42, 1574 (1971).

54. C. F. Coll and A. B. Harris, Phys. Rev. 4B, 2781 (1971).

55. L. I. Amstutz, H. Meyer, S. M. Myers, and D. C. Rorer, Phys. Rev. 181, 589 (1969).

56. W. N. Hardy, I. F. Silvera, and J. P. McTague, Phys. Rev. Letters 22, 297 (1969).

57. S. C. Durana and J. P. McTague, Phys. Rev. Letters 31, 990 (1973).

58. E. W. Albers, P. Hartech, and R. R. Reeves, J. Amer. Chem. Soc. 86, 204 (1964).

59. R. Frauenfelder, F. Heinrich, and J. B. Olin, Helv. Phys. Acta 38, 279 (1965).

60. R. R. Stone, Measurement of Laser Fusion Capsules Using the Interferometer Method of Excess Fractions, Lawrence Livermore Laboratory, Rept. UCRL-51788 (1975).

61. B. Weinstein, Lawrence Livermore Laboratory, private communication, 1975.

62. R. R. Stone and P. C. Souers, paper to be published.

63. P. C. Souers, paper to be published.

64. J. Dyson, Interferometry as a Measuring Tool (Machinery Publishing Co., London, 1970), pp. 96-98, 103-111.

65. R. P. Reedy, Nondestructive Testing of Laser Targets, Lawrence Livermore Laboratory, Rept. UCRL-51630 (1974).

66. R. P. Reedy, paper to be published in the Journal of Applied Physics.

WEC/nus